Near-bandedge cathodoluminescence of an AlN homoepitaxial film

E. Silveira[a] and J. A. Freitas, Jr.[b]
Naval Research Laboratory, ESTD, Washington, DC 20375-5347

M. Kneissl, D. W. Treat, and N. M. Johnson
Palo Alto Research Center, Palo Alto, California 94304

G. A. Slack[c] and L. J. Schowalter[c]
Crystal IS, Inc., Latham, New York 12110

(Received 23 September 2003; accepted 12 March 2004; published online 20 April 2004)

Cathodoluminescence experiments were performed on a high-quality AlN epitaxial film grown by organometallic vapor phase epitaxy on a large single crystal AlN substrate. The low-temperature near-bandedge spectra clearly show six very narrow lines. The thermal quenching behavior of these emission lines provides insight on how to assign them to free and bound exciton recombination processes. The binding energy for the free-exciton-*A* in AlN was found to be nearly twice that in GaN. The observation of the free-exciton-*A* first excited state permitted us to estimate its reduced effective mass and, by using recent reported values for the hole effective mass in Mg-doped AlN, the electron effective mass in AlN has been deduced. © *2004 American Institute of Physics.* [DOI: 10.1063/1.1738929]

AlN is a natural substrate for III-nitride device layers, based on its crystal structure and chemical and thermal compatibility with GaN epilayers. Due to the previous lack of high quality material and the difficulties associated with the optical measurements in the UV range only a few reports of near-band-edge (NBE) UV emission on wurzite type AlN films on SiC, sapphire or Si substrates can be found in the literature,[1–8] and an even smaller number have been reported for bulk AlN.[9–12] Additional experimental work is needed to address the controversy about important material parameters of AlN, as for example, values for the carrier effective masses[13–15] and the dielectric constant.[16–18]

In this letter we report on the results of our cathodoluminescence (CL) studies of a high quality wurzite type AlN film homoepitaxially grown on a large single crystal AlN wafer. The CL measurements were carried out at different temperatures for a fixed electron beam energy density value. The beam current was held at 5 μA, and the voltage at 10 kV. The energy density was about 700 W/cm^2.

The high quality, large, bulk AlN single crystals, used here as substrates, were grown by a sublimation-recondensation technique. Triple-crystal x-ray diffraction experiments conducted on similar bulk AlN samples have shown a full width at half maximum (FWHM) of less than 10 arcsec for the rocking curve. More details can be found elsewhere.[19,20] The substrate crystal was 287 μm thick. The homoepitaxial AlN films have been grown by organometallic vapor phase epitaxy on the single crystal AlN substrates. Every effort was made to produce a high-purity, low oxygen content film. The oxygen concentration has a large influence on the CL intensities of the NBE emissions as studied by Slack *et al.*[10] The substrates used in our experiment are similar to sample 00G of Ref. 10, where the oxygen concentration in that sample was as low as 4.9×10^{19} atoms/cm^3, measured by neutron activation. This value can be seen as an upper limit for the substrates, once the intensity ratio between the NBE emissions and the defect lower energy band have improved for samples recently fabricated. Since the intensity ratio between the NBE emissions and the defect lower energy band for the homoepitaxial film is very similar to the ones observed for the substrates, it is fair to assume the value already mentioned for the O concentration in our bulk AlN as the upper limit for the film as well. The vector normal to its surface is misaligned by 10° from the *c* axis. The film thickness is nominally 0.5 μm, which is somewhat larger than the penetration depth of the *e*-beam typically used in this experiment.[21] An accurate characterization of the film structure, impurity, and defect content is in progress and will be reported in the near future.

Figure 1 shows a low-temperature CL spectrum of the AlN film measured at high resolution in the near-band-edge energy range. The hollow squares represent the experimental data taken at 5 K, while the full line curve is our best fit to the experimental data using Lorentzian line shapes. The six transitions clearly observed are represented separately by the dashed lines, which add up to the full line curve. The energy positions and full widths at half maxima (FWHM) of all six

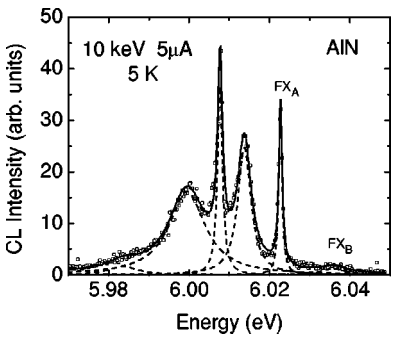

FIG. 1. High resolution CL spectrum of an AlN homoepitaxial film. The full line represents our best fit using Lorentzian line shapes and the dashed lines are the transitions composing the full line.

[a]Also at: Depto. de Fisica, UFPR, CP19044, Curitiba-PR, Brazil.
[b]Electronic mail: jaime.freitas@nrl.navy.mil
[c]Also at: Rensselaer Polytechnic Institute, Troy, NY 12180.

TABLE I. Energy positions, full widths at half maxima (FWHM), and tentative assignments for the peaks shown in Fig. 1.

E (eV)	FWHM (meV)	Assignments
5.984	9.4	$A_?{}^0X_A$
6.000	11.0	$D_{2?}{}^0X_A$
6.008	1.5	$D_{1?}{}^0X_A$
6.014	4.0	$D_{1?}{}^0X_B$
6.023	1.0	FX_A
6.036	8.0	FX_B

curves are summarized in Table I. The assignments have been made based on thermal quenching studies and will be discussed below. The FWHM of the narrowest emission line at 6.023 eV is about 1.0 meV and may be limited by our spectrometer resolution for the slit size used during the experiment. A measurement of the 253.65 nm emission line of a low-pressure Hg-lamp using the same slits size set resulted in a FWHM of about 0.7 meV. The linewidths observed here are quite small and are comparable with the ones observed on bulk AlN grown by thermodecomposition of $AlCl_3{\cdot}NH_3$ and on AlN grown by the sublimation-recondensation technique reported recently.[11,12]

As similar structures have been observed in the past in the photoluminescence (PL) spectra of high quality GaN samples, we show in Fig. 2(a) the NBE transitions for a thick, freestanding GaN sample. In the spectrum of Fig. 2(a) we observe emission lines attributed to the free-exciton-A (FX_A), free-exciton-B (FX_B), the dominant exciton bound to a neutral donor (X-D^0) and the two-electron-satellites region (2ES). Details of the measurements and line assignments in GaN can be found elsewhere.[22,23] The structure named as FX_A^2 is attributed to the excited states of the free-exciton-A.[22] Figure 2(b) shows the CL spectra for the AlN film as a function of temperature, which have been multiplied by various constant factors to remove overlap and to permit a better visualization. Note that the energy scale is twice that shown in Fig. 2(a). We observe a rapid decrease of the intensities of the four peaks initially seen between 5.98 and 6.01 eV with increasing temperature. This is typical behavior of recombination process involving excitons bound to shallow neutral centers. The peaks at 6.023 and 6.036 eV remain the most intense spectral features with increasing temperature. We tentatively attribute these two peaks to the so-called free-exciton-A (FX_A) and free-exciton-B (FX_B), respectively, since they are expected to dominate the emission spectrum at high temperature, due to their higher binding energies. Although their intensities decline little with increasing temperature they dominate the higher temperature spectra at the expenses of the thermal dissociation of the bound exciton-neutral-donor complexes that set the excitons free. The line around 6.07 eV, represented here also as FX_A^2, is two orders of magnitude weaker than the most intense bands of the spectrum. Based on the similarity of the luminescence spectra of both GaN and AlN we assume that the peak at 6.07 eV observed in our AlN sample is the first excited state of the FX_A, and consequently we estimate the FX_A binding energy as 63 meV. Note that this is almost twice as large as the binding energy observed for the FX_A in GaN.[22]

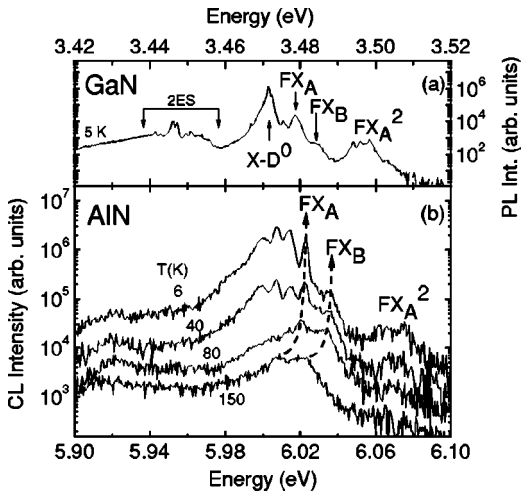

FIG. 2. (a) PL spectrum of a thick, freestanding GaN sample. Indicated are the free-exciton-A (FX_A), free-exciton-B (FX_B) and the excited state of the FX_A (FX_A^2). The X-D^0 represents an exciton bound to a neutral donor and 2ES is the two-electron satellites region; (b) temperature dependence of the AlN film CL spectra at the NBE range.

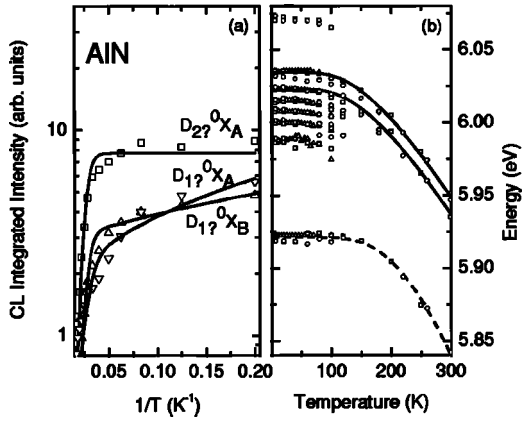

FIG. 3. (a) Effect of temperature on the integrated intensities of the peaks attributed to bound excitons. The full lines represent the best fitting to the data; (b) energy positions of the peaks from Fig. 2(b) as a function of temperature. The full lines in (b) represent the Bose–Einstein relation for the energy as a function of temperature.

There is considerable controversy in regards to the calculated effective mass values[13–15] and to the measured values of the static dielectric constant (7.34–9.14)[16,17] for AlN. Assuming a hydrogenic expression for the free-exciton binding energy and using the two values mentioned for the dielectric constant as the limits, we find in our case a value for the reduced effective mass of the free-exciton ranging from 0.25 to $0.39m_0$. The average hole effective mass in AlN was recently estimated to be between 2.02 and $3.13m_0$, based on experimental measurements of the Mg acceptor binding energy in Mg-doped AlN epilayers,[8] the effective mass theory and the dielectric constant values mentioned earlier.[16,17] Using these reported hole effective mass values in combination with our experimental results, we estimate that the electron effective mass in AlN spans from 0.29 to $0.45m_0$, depending on the dielectric constant value used in the calculation. The values for the electron effective mass deduced here agrees well with the most common values between 0.27 and $0.35m_0$.[13–15]

Our thermal quenching studies of the high resolution spectrum represented in Fig. 3(a) lead to binding energies of about 21, 15, and 23 meV for the lines at 6, 6.008, and 6.014

eV, respectively. The intensity behavior of the lines at 6.023 and 6.036 eV have been left out of this figure for the sake of clarity, once their integrated intensities decline by a factor lower than 2 for the same temperature range. The line at 6.008 eV is very close in energy to the line that Freitas *et al.*[11] assigned to the recombination process in AlN associated with the annihilation of *A* excitons bound to a shallow neutral donor. Based on the similarity of both spectral energies and binding energy values we tentatively attribute the lines at about 6, 6.008, and 6.014 eV to unknown neutral donor-bound-exciton recombinations, represented by $D_{2?}{}^0X_A$, $D_{1?}{}^0X_A$, and $D_{1?}{}^0X_B$. Similar results have also been reported for bulk AlN,[12] crystals of which have been used as the substrate for the homoepitaxial growth of the film discussed in this letter. The presence of multiple donors incorporated during growth has been recently reported on thick, high-quality, unintentionally doped freestanding GaN films fabricated by hydride-vapor-phase epitaxy (HVPE).[23] The different binding energies of the donor-bound excitons, determined from photoluminescence, are proportional to the neutral donor binding energies, as measured by Fourier transform infrared (FTIR) measurements. Besides that, based on the similarity between the PL spectra of HVPE GaN and the CL spectra of our AlN homoepitaxial layer, highlighted in Figs. 2(a) and 2(b), the transition at about 6.014 eV may be attributed to *B* excitons bounded to the same donor mentioned previously, $D_{1?}{}^0X_B$, or to *A* excitons bound to a shallower donor. The lines at 6.000 and 5.984 eV could be assigned to a different donor and to an acceptor, respectively, but since little is known about the chemical nature of the impurities in AlN these assignments will require further study.

In Fig. 3(b) the positions of the peaks observed in Fig. 2(b) are presented as a function of temperature. Different symbols represent different measurements. The full lines in Fig. 3(b) represent the Bose–Einstein fitting for the temperature variation of the band gap. The empirical description of the band-gap variation assuming Bose–Einstein statistics gives a better result for polar semiconductors in which the optical and acoustical phonon branches are energetically close.[24] This same description was used in the past for the temperature dependence of the GaN band gap.[25] For the curves associated with free-excitons *A* and *B* the same set of parameters have been used. The nearly linear behavior for temperatures above 200 K with a slope of about -0.54 meV/K is very close to previously reported values for bulk AlN (Ref. 9) and AlN films.[2,5]

An additional band at about 5.920 eV can be seen in Fig. 2(b). Similar bands observed in bulk AlN were previously assigned to LO-phonon replicas.[9] As we can see in Fig. 3(b) its temperature dependence is somewhat different from the two lines that we call donor-bound-exciton lines. Moreover the difference in the energy positions between this band and that attributed to the donor-bound-excitons at 6.008 and 6.014 eV do not match the phonon energies measured for bulk AlN.[11] Therefore, we attribute this emission line to a defect band or to LO-phonon assisted emission edge of free excitons,[26] rather than to a LO-phonon replica.

In conclusion, six emission lines between 5.98 and 6.03 eV are distinguishable in the low-temperature NBE spectra of our AlN films. These lines are considerably narrower than those previously observed. Cathodoluminescence measurements carried out at different temperatures provide evidence to support the assignment of the lines to free- and bound-exciton recombination processes. The observation of the free-exciton-*A* first excited state yields a binding energy of 63 meV for the free-exciton-*A* for AlN. In addition we estimate its effective reduced mass between 0.25 and $0.39m_0$. Furthermore, we deduce an electron effective mass value from 0.29 to $0.45m_0$ based on recently reported experimental results of the hole effective mass. A more accurate value for the dielectric constant is needed to reduce the uncertainty in the carrier effective mass.

The work at NRL was partially supported by the ONR-IFO (Grant No. N00014-02-1-4087) and by ONR (Contract No. N00014WR20015) monitored by Dr. C. E. C. Wood. The work at PARC was partially supported by the DARPA-SUVOS Program under SPAWAR Systems Center Contract No. N66001-02-C-8017. The work at Crystal IS was partially supported by DARPA Contract No. F33615-02-C-5417 monitored by J. Blevins and Dr. E. Martinez.

[1] C.-M. Zetterling, M. Östling, K. Wongchotigul, M. G. Spencer, X. Tang, C. I. Harris, N. Nordell, and S. S. Wong, J. Appl. Phys. **82**, 2990 (1997).
[2] X. Tang, F. Hossain, K. Wongchotigul, and M. G. Spencer, Appl. Phys. Lett. **72**, 1501 (1998).
[3] Y. Shishkin, R. P. Devaty, W. J. Choyke, F. Yun, T. King, and H. Morkoç, Phys. Status Solidi A **188**, 591 (2001).
[4] N. Teofilov, K. Thonke, R. Sauer, D. G. Ebling, L. Kirste, and K. W. Benz, Diamond Relat. Mater. **10**, 1300 (2001).
[5] T. Onuma, S. F. Chichibu, T. Sota, K. Asai, S. Sumiya, T. Shibata, and M. Tanaka, Appl. Phys. Lett. **81**, 652 (2002).
[6] J. Li, K. B. Nam, M. L. Nakarmi, J. Y. Lin, and H. X. Jiang, Appl. Phys. Lett. **81**, 3365 (2002).
[7] K. B. Nam, J. Li, M. L. Nakarmi, J. Y. Lin, and H. X. Jiang, Appl. Phys. Lett. **82**, 1694 (2003).
[8] K. B. Nam, M. L. Nakarmi, J. Li, J. Y. Lin, and H. X. Jiang, Appl. Phys. Lett. **83**, 878 (2003).
[9] E. Kuokstis, J. Zhang, Q. Fareed, J. W. Yang, G. Simin, M. Asif Kahn, R. Gaska, M. Shur, C. Rojo, and L. Schowalter, Appl. Phys. Lett. **81**, 2755 (2002).
[10] G. A. Slack, L. J. Schowalter, D. Morelli, and J. A. Freitas, Jr., J. Cryst. Growth **246**, 287 (2002).
[11] J. A. Freitas, Jr., G. C. B. Braga, E. Silveira, J. G. Tischler, and M. Fatemi, Appl. Phys. Lett. **83**, 2584 (2003).
[12] E. Silveira, J. A. Freitas, Jr., G. A. Slack, and L. J. Schowalter, Phys. Status Solidi C **0**, 2618 (2003).
[13] M. Suzuki and T. Uenoyama, Phys. Rev. B **52**, 8132 (1995).
[14] S.-H. Wei and A. Zunger, Appl. Phys. Lett. **69**, 2719 (1996).
[15] K. Kim, W. R. L. Lambrecht, and B. Segall, Phys. Rev. B **56**, 7363 (1997).
[16] A. T. Collins, E. C. Lightowlers, and P. J. Dean, Phys. Rev. **158**, 833 (1967).
[17] T. L. Chu and R. W. Keln, Jr., J. Electrochem. Soc. **122**, 995 (1975).
[18] T. Wethkamp, K. Wilmers, C. Cobet, N. Esser, W. Richter, O. Ambacher, M. Stutzmann, and M. Cardona, Phys. Rev. B **59**, 1845 (1999).
[19] L. J. Schowalter, Y. Shusterman, R. Wang, I. Bhat, G. Arunmozhi, and G. A. Slack, Appl. Phys. Lett. **76**, 985 (2000).
[20] J. C. Rojo, L. J. Schowalter, R. Gaska, M. Shur, M. A. Khan, J. Yang, and D. D. Koleske, J. Cryst. Growth **240**, 508 (2002).
[21] T. E. Everhart and P. H. Hoff, J. Appl. Phys. **42**, 5837 (1971).
[22] A. V. Rodina, M. Dietrich, A. Göldner, L. Eckey, A. Hoffmann, Al. L. Efros, M. Rosen, and B. K. Meyer, Phys. Rev. B **64**, 115204 (2001).
[23] J. A. Freitas, Jr., W. J. Moore, B. V. Shanabrook, G. C. B. Braga, S. K. Lee, S. S. Park, and J. Y. Han, Phys. Rev. B **66**, 233311 (2002).
[24] Q. Guo, M. Nishio, and H. Ogawa, Phys. Rev. B **64**, 113105 (2001).
[25] K. P. Korona, A. Wysmolek, K. Pakula, R. Stepniewski, J. M. Baranowski, I. Grzegory, B. Lucznik, M. Wroblewski, and S. Porowski, Appl. Phys. Lett. **69**, 788 (1996).
[26] B. V. Shanabrook, S. Rudin, T. L. Reinecke, W. Tseng, and P. Newman, Phys. Rev. B **41**, 1577 (1990).